

## Further Studies of the Structure and Stability of Burner Flames

Guenter von Elbe and Morris Mentser

Citation: *The Journal of Chemical Physics* **13**, 89 (1945); doi: 10.1063/1.1724004

View online: <http://dx.doi.org/10.1063/1.1724004>

View Table of Contents: <http://scitation.aip.org/content/aip/journal/jcp/13/2?ver=pdfcov>

Published by the [AIP Publishing](#)

---

### Articles you may be interested in

[Burner for Making Kinetic Measurements in Flames](#)

Rev. Sci. Instrum. **33**, 766 (1962); 10.1063/1.1717963

[Stability and Structure of Bunsen Flame](#)

J. Chem. Phys. **22**, 1784 (1954); 10.1063/1.1739908

[Vortex Burner—A Useful Tool for Studying the Flame Stability of Gaseous Fuels and Fuel Mixtures](#)

Rev. Sci. Instrum. **25**, 418 (1954); 10.1063/1.1771090

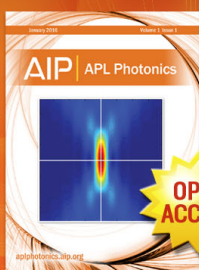
[Further Studies of Hydrocarbon Flame Spectra](#)

J. Chem. Phys. **18**, 763 (1950); 10.1063/1.1747757

[Stability and Structure of Burner Flames](#)

J. Chem. Phys. **11**, 75 (1943); 10.1063/1.1723808

---



Launching in 2016!

The future of applied photonics research is here

OPEN  
ACCESS

**AIP** | APL  
Photonics

Further Studies of the Structure and Stability of Burner Flames<sup>1-3</sup>

GUENTHER VON ELBE AND MORRIS MENTSER

*Central Experiment Station, Bureau of Mines, Pittsburgh, Pennsylvania*

(Received September 23, 1944)

It is shown that, contrary to Mache's model of the progressive extinction of a flame<sup>4</sup> from the burner rim, a combustion zone cannot vanish within a combustible stream. The depth of penetration of the quenching of the explosive reaction by the burner wall is calculated from values of burning velocity and critical boundary velocity gradient for flashback; it is compared with the limiting distance between plane-parallel plates and the limiting tube diameter for flame propagation. The thermal expansion of the gas normal and parallel to the combustion zone is discussed. An experimental analysis and discussion of partial entrance of the combustion zone into the burner tube (tilted flame) and partial attachment to the burner rim are given. New data have been obtained on hydrogen and acetylene flames. For instantaneous flashback, the boundary velocity gradients are independent of tube diameter, as expected; these gradients are not a satisfactory criterion for flame stability because flashback can be readily induced by tilted flames. The limit of the tilted-flame range is represented by the semitheoretical equation

$$g/(1-4S_u/gR)^{\frac{1}{2}} = \text{const.}$$

$g$  is the boundary-velocity gradient,  $S_u$  the burning velocity, and  $R$  the tube diameter. The boundary-velocity gradients for blow-off are again found constant over the laminar flow range. The compression of acetylene-oxygen streams by the combustion zone has been measured. The burning velocities calculated from these and additional thermodynamic data agree well with those determined from gas flow and cone surface.

**I**N a previous paper,<sup>4</sup> the flashback and blow-off of burner flames, the pattern of the gas flow, and the distribution of gas velocity and temperature have been investigated theoretically and experimentally. The experiments were made with mixtures of natural gas and air. The present paper contains additional observations on flames of mixtures of hydrogen and acetylene with air and oxygen, and a discussion of several points that have not been fully treated before.

In this, as in the previous paper, the term "combustion zone" is synonymous to the frequently used terms "explosion wave" or "flame front." It denotes the narrow preheating and reaction zone which separates the burned from the unburned gas. Within the zone, in the layers adjacent to the completely burned gas, heat is released and atoms and free radicals are formed by the chemical reaction; a part of the heat and active species (chain carriers) is transferred by

conduction and diffusion to the adjoining layers of unburned gas which in turn become activated to rapid chemical reaction. In this way, the combustion zone progresses against the unburned gas at a definite velocity  $S_u$ , the burning velocity, whose magnitude is evidently affected by any factors which modify the reaction rate and the rates of heat transfer and diffusion into the unburned gas. Thus, at a certain distance from a solid wall, the burning velocity decreases to zero, and this distance becomes smaller as the temperature of the wall is raised.

The combustion zone is generally plainly visible owing to chemiluminescence, notably by emission of CC and CH bands; and if the zone retains a fixed position against a gas stream issuing from a burner port, it forms the well-known inner flame cone.

#### I. SUPPLEMENTAL DISCUSSION OF THE STABILITY AND STRUCTURE OF BURNER FLAMES

##### (A) The Propagation and Structure of the Combustion Zone

While the work of Mache<sup>5</sup> has materially contributed to the theory of burner flames, it appears

<sup>5</sup> H. Mache, *Die Physik der Verbrennungserscheinungen* (Veit und Comp., Leipzig, 1918), pp. 25-54.

<sup>1</sup> Published by permission of the Director, Bureau of Mines, U. S. Department of the Interior.

<sup>2</sup> From a thesis submitted by Morris Mentser to the faculty of the Graduate School of the University of Pittsburgh in partial fulfillment of the requirements for the degree of Master of Science.

<sup>3</sup> Contribution from the Central Experiment Station, Bureau of Mines, U. S. Department of the Interior.

<sup>4</sup> B. Lewis and G. von Elbe, *J. Chem. Phys.* **11**, 75 (1943).

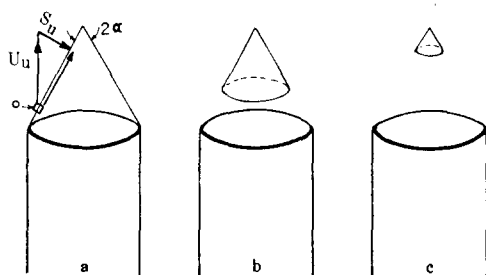


FIG. 1. Illustration of Mache's concept of progressive extinction of the combustion zone from the rim of the burner port.

that neither this author nor subsequent investigators have taken sufficient account of the mechanism of propagation of the combustion zone. Thus, an erroneous concept has persisted in the literature regarding a supposed tendency of the burner flame to extinguish itself progressively from the rim toward the stream axis. This is illustrated in Fig. 1. For simplicity, the gas velocity  $U_u$  is taken as uniform over the cross section of the stream issuing from the burner port. An inner cone is supposed to have been formed with an opening angle  $2\alpha$  so that  $S_u = U_u \sin \alpha$ ; that is, the burning velocity is everywhere equal to the normal component of the gas velocity, and a necessary condition for the stability of the cone is thus fulfilled. It is now further argued that any element of the combustion zone (as, for example, the element at point O) is simultaneously carried upward by the gas flow with the velocity  $U_u$  and inward by the combustion with the velocity  $S_u$  and that consequently the element moves along the resultant of the vectors  $U_u$  and  $S_u$  within the cone surface at a velocity  $U_u \cos \alpha$ . On this basis it would appear, as illustrated according to Mache in Figs. 1b and 1c, that an element at the rim moves within the combustion zone toward the cone tip; that is, the cone is progressively extinguished from the rim toward the tip. To maintain a stationary cone, Mache assumes that the combustion zone is continually restored at the cone base by a virtual pilot flame which is maintained by a supposed slow-moving, turbulent boundary layer surrounding the gas stream.

To visualize the consequences of this concept, consider an elementary tube extending normal

to the combustion zone from the element O into the unburned gas. This tube encloses all the gas elements that enter the combustion zone successively at points above O, and the tube moves correspondingly upward. Since, in the absence of a pilot flame at the cone base, the gas at lower points is supposed to remain unignited, it is virtually assumed that the reaction-inducing flow of heat and chain-carriers from the successively burning gas elements propagates only within the tube. This is certainly not the case. Rather, the progress of a combustion zone may be visualized in accordance with the principles of Huygen's construction for the propagation of a wave front, as shown schematically in Fig. 2A. A gas element entering the combustion zone is activated to rapid chemical reaction by contributions of heat and chain-carriers, not only from the preceding gas element in the same stream tube, but also from gas elements in the adjoining stream tubes; in turn it activates, not only the succeeding gas element in its own stream tube, but also the elements in adjoining stream tubes. Thus, ignition spreads from any point of the combustion zone laterally as well as forward; accordingly, a combustion zone cannot vanish within a combustible stream as Fig. 1 would indicate; rather, it always tends to occupy the whole cross section of the stream and moves as a unit with or against the stream or remains stationary, as the case may be. The combustion zone moves with the stream—the flame blows off—when the gas velocity everywhere exceeds the burning velocity; it moves against the stream—the flame flashes back—when the burning

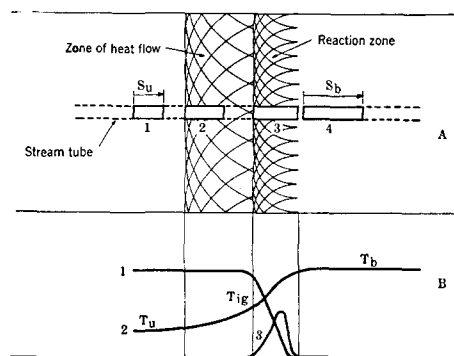


FIG. 2. A. Schematic view of the combustion zone. B. Temperature and concentration gradients within the combustion zone. 1. Concentration of fuel gas. 2. Temperature. 3. Concentration of atoms and free radicals.

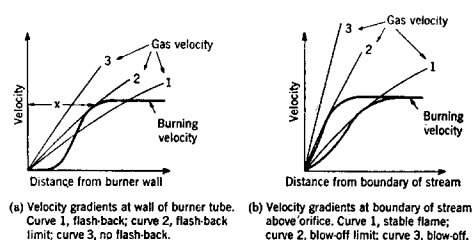


FIG. 3. Illustration of flashback and blow-off conditions.

velocity exceeds the gas velocity at any one point; and the flame remains stationary when the burning velocity equals the gas velocity at any one point but does not exceed it anywhere.

Other details of the combustion zone that are shown schematically in Fig. 2 are self-explanatory. In accordance with previous practice, the subscripts  $u$  and  $b$  refer to unburned and burned gas, respectively. The temperature at the beginning of the zone of active chemical reaction may be referred to as the ignition temperature  $T_{ig}$ ; it obviously bears little relation to the ignition temperatures determined by heating or adiabatically compressing a combustible mixture to the point of explosion because the ignition process is controlled by other factors besides temperature.

### (B) Depth of Penetration of the Quenching of the Explosive Reaction by the Burner Wall

It has been shown previously that a burner flame remains stable between two critical values of the gradient of gas velocity at the stream boundary.<sup>4</sup> For laminar flow in cylindrical tubes the gradient  $g$  may be written as a function of the total gas flow  $V$  and the radius  $R$ ,

$$\lim_{r \rightarrow R} \left( \frac{-dU}{dr} \right) = g = 4V/\pi R^3. \quad (1)$$

If subscripts  $F$  and  $B$  refer to the flashback and blow-off condition, respectively, then  $g_F$  and  $g_B$  are the lower and upper critical values of the velocity gradient between which the flame is stable. The conditions near the stream boundary are illustrated in Figs. 3a and 3b. The values of  $g_F$  and  $g_B$  obviously represent the slopes of the gas velocity curves 2 in the corresponding diagrams. With reference to Fig. 3a, the distance  $X$  from the wall over which the burning velocity is

below its normal value may be defined as the depth of penetration of the quenching of the explosive reaction by the burner wall. It can be calculated approximately from measured values of  $g_F$  and  $S_u$  by assuming that, at the point of contact of the curves of burning velocity and critical gas velocity, the burning velocity is close to its normal measured value. It then follows that

$$X = S_u/g_F. \quad (2)$$

The value  $X$  may be considered a measure for the limiting distance between plane parallel plates and, correspondingly, for the limiting diameter of cylindrical tubes below which flame propagation is quenched. The validity is only approximate, since  $X$  refers to a single wall bordering on a large volume of gas, whereas the quenching effects of two opposing walls merge and augment each other. Hence, the limiting

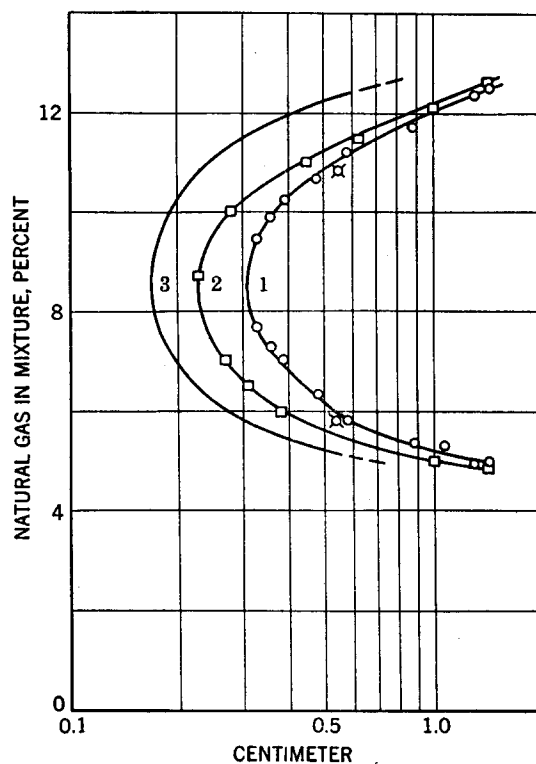


FIG. 4. Depth of penetration of the quenching of the explosive reaction by the burner wall. Natural gas-air mixtures. Curve 1, limiting diameter of cylindrical tubes for downward flame propagation ( $\circ$  data by Lewis and von Elbe;  $\square$  new data). Curve 2, limiting distance between plane parallel plates for downward flame propagation. Curve 3, depth of penetration calculated from critical velocity gradients for flashback.

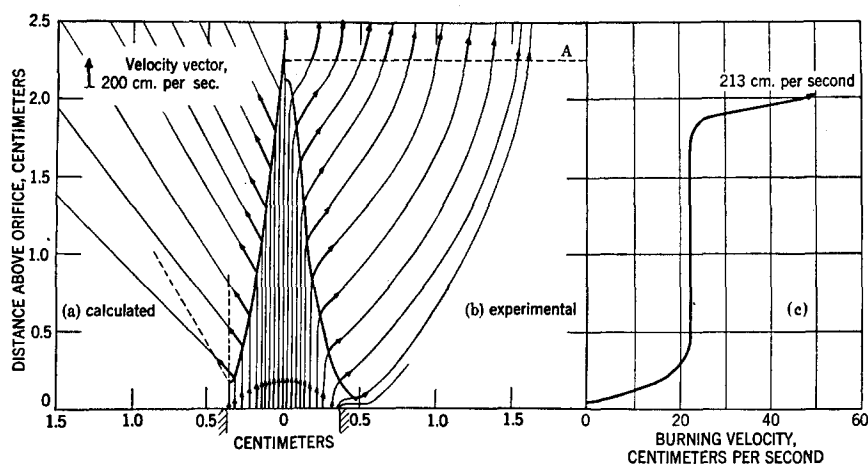


FIG. 5. Diagram of vertical center plane of natural gas-air flame on rectangular burner tube of  $0.755 \times 2.19$  cm cross section. Mixture composition, 7.5 percent natural gas; flow, 204 cubic centimeters per second. (a) and (b): Combustion zone and flow pattern. (c) Burning velocity.

distance between plane parallel plates is larger than  $X$  and may, in the absence of a quantitative theory, be estimated to be comparable to  $2X$ . The limiting diameter of cylindrical tubes is even larger because of the additional effect of curvature. This is illustrated in Fig. 4. Curve 1 represents previously obtained data<sup>4</sup> with two new points added in order to insure that the composition of the natural gas had not changed appreciably in the interval between previous and present experiments. Curve 2 represents observations on a burner formed by two plane parallel plates, one fixed and the other movable. Curve 3 represents values of  $2X$  calculated from previously published data of  $g_F$  and  $S_u$ .<sup>4</sup> It is seen that the limiting distance between plane parallel plates is even larger than  $2X$ , although not greatly so. The data of Fig. 4 refer to walls at room temperature; as the temperature is increased, the depth of penetration decreases.

It is of interest to report an observation by F. A. Smith<sup>6</sup> that a mixture of  $2H_2 + O_2$  flashed back in a cold glass tube of 0.013-inch (0.033-cm) diameter. For this mixture  $g_F$  is found to be  $1.3 \times 10^5 \text{ sec}^{-1}$  (see Fig. 8) and  $S_u$ , according to Jahn,<sup>7</sup> is 870 cm per second. The value of  $X$  is, therefore, 0.0067 cm which accords well with Smith's observation.

<sup>6</sup> *Combustion* (American Gas Association, New York, 1932), 3rd edition, p. 110.

<sup>7</sup> G. Jahn, *Der Zündvorgang in Gasgemischen* (Oldenbourg, Berlin, 1934), p. 21.

### (C) Modification of the Gas Flow at Tip and Base of the Conical Combustion Zone

In Fig. 5, a previous analysis<sup>4</sup> of a flame cone and flow pattern is reproduced with an additional curve showing the change of burning velocity over the cone surface. The analysis shows that the gas elements that enter the combustion zone in the range of constant burning velocity between tip and base expand only in the direction normal to the zone. At the tip and base, however, thermal expansion also takes place parallel to the combustion zone. In the axial stream tube, the expansion appears to be almost completely of the latter type, since the experimental records of this and other flames show that there is no appreciable change of gas velocity between unburned and burned gas in the central flow line. This lateral expansion at the cone tip is made possible by the divergence of the flow lines caused by refraction in the combustion zone. At the base the expanding gas elements acquire considerable velocity components parallel to the combustion zone in the direction of the free atmosphere. This is clearly shown by the outermost flow lines of Fig. 5b. Since the acceleration of the gas elements results in opposing inertia forces, the expansion parallel to the combustion zone in the inner flow lines is gradually checked, and thermal expansion normal to the zone predominates.

In the original photographs, the flow lines are

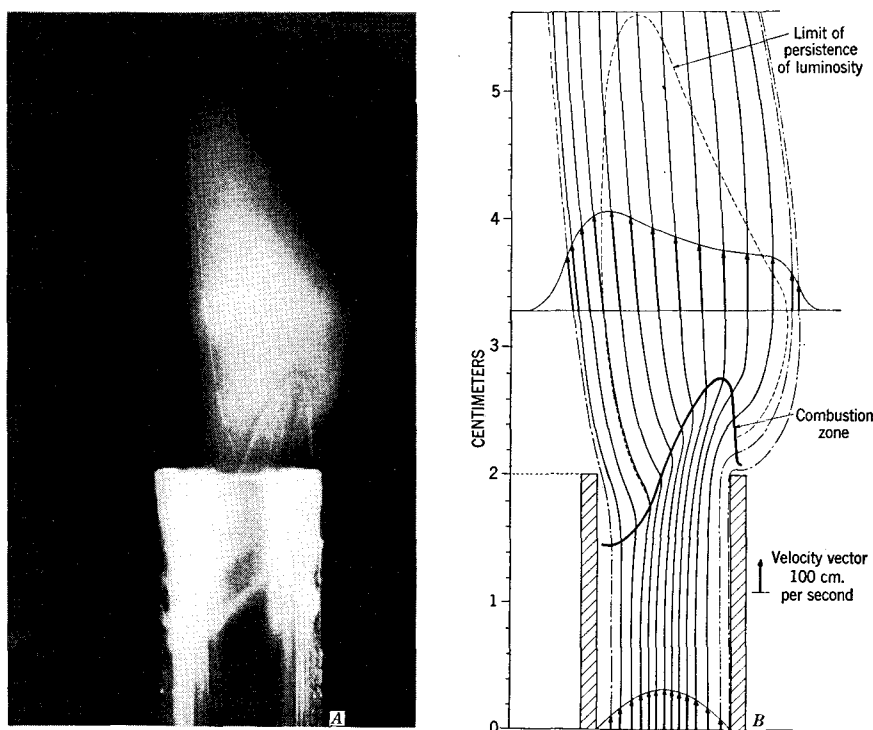


FIG. 6. Flame of natural gas and air, partially drawn into burner tube at gas flow just exceeding critical flow for flashback. Mixture composition, 8.1 percent natural gas in air; gas flow, 52 cc per second; inside diameter of tube, 1.068 cm. A. Photograph with particle tracks in vertical center plane (cf. Lewis and von Elbe, reference 4). B. Diagram of flow pattern and velocity distribution. Solidly-drawn flow lines are so located that the mass flow between any two adjoining lines is the same.

seen to diverge slightly even before entering the heating zone. It may be remembered that the combustion zone exerts a pressure on the unburned gas because of the acceleration of the gas flow.<sup>5</sup> This acceleration is smaller at the base of the cone than elsewhere because the burning velocity there is lower. Consequently, there exists a pressure drop in the unburned gas below the combustion zone from the stream center to the burner rim which appears to be the cause of the observed divergence of the flow lines.

#### (D) The Tilted Flame

A flame form, frequently observed when the gas flow is gradually reduced toward the flashback condition, is typified by the diagram in Fig. 6. It has already been described briefly.<sup>4</sup> The dynamic symmetry of the gas stream is destroyed: The combustion zone has partly entered the burner tube and exerts a pressure normal to the tube axis which causes a deflection

of the stream of unburned gas in the opposite direction. The resulting change of velocity distribution in the unburned gas causes a decrease of the boundary velocity gradient, below the critical flashback value, in the region where the flame penetrates into the tube; this permits the combustion zone to propagate against the stream. As the combustion zone travels downward, the resistance of the flow of unburned gas to the deflecting pressure increases until a position of equilibrium is reached, in which the boundary velocity gradient at the deepest point of penetration has become equal to the critical gradient for flashback, but exceeds the critical value at lower points in the burner tube. Obviously, the equilibrium position is maintained only when the burner tube is cooled sufficiently. Generally, as the tube temperature increases, the combustion zone continues to travel downward, and flashback results.

When the gas flow is gradually increased

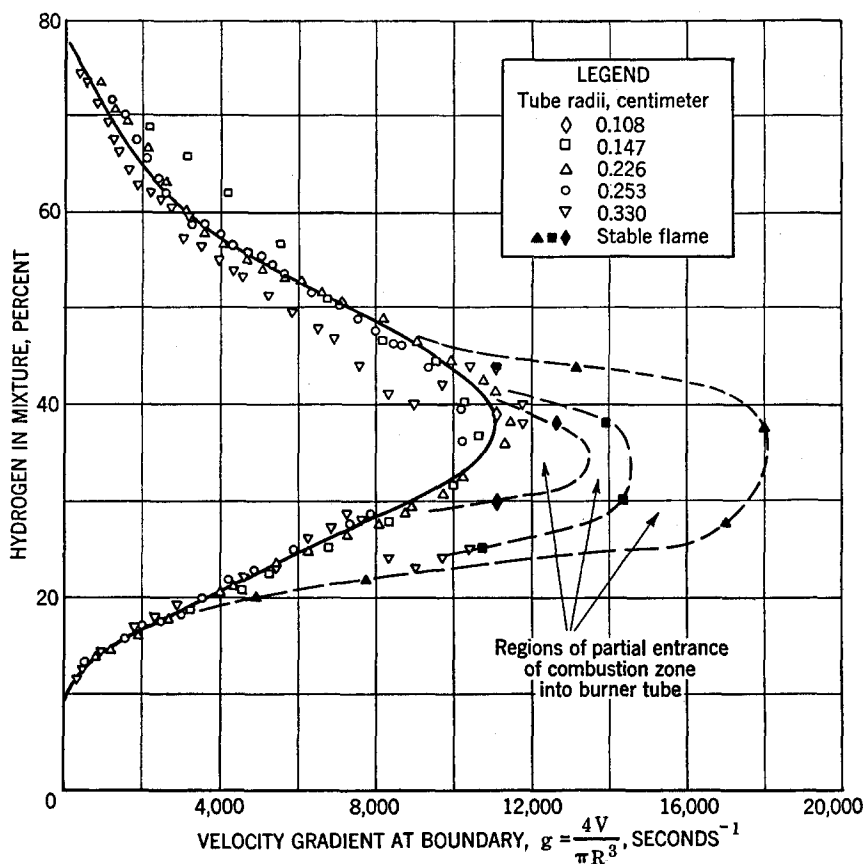


Fig. 7. Critical velocity gradients at boundary of gas stream for flashback of hydrogen-air flames in cylindrical water-cooled tubes of different diameters.

toward the blow-off condition, the combustion zone often remains attached to the port rim at a single point and extends from there at a steep angle over the gas stream. The phenomenon is analogous to the foregoing: The pressure exerted by the combustion zone deflects the flow lines in the unburned gas so that the boundary velocity gradient at the point of attachment is smaller than the critical gradient for blow-off. At all other points along the port rim, the critical gradient is exceeded. On further, usually slight, increase of the gas flow, the flame blows off completely.

Tilted flames, such as are shown in Fig. 6, are formed only below some critical flow which is a function of tube diameter. It is obviously desirable to determine this function theoretically, but the problem appears to be rather difficult and has not been completely solved. Nevertheless, it has been found possible to arrive at a

semi-empirical equation with the aid of theoretical considerations. The equation is given in the following experimental part of the paper.

## II. EXPERIMENTS ON HYDROGEN AND ACETYLENE FLAMES

### (A) Apparatus and Procedure

The two gases, comprising the gas mixture to be studied, were passed individually through calibrated flowmeters into a mixing chamber. Effective mixing was accomplished by directing the two jets in the chamber at a right angle against each other (see, for example, Rummel<sup>8</sup>). On leaving the chamber, the gas mixture entered directly into a vertically mounted burner tube whose tip was surrounded by a water jacket. The gas was ignited by approaching the stream near the rim of the tube with a small flame.

<sup>8</sup> K. Rummel, *Der Einfluss des Mischvorganges auf die Verbrennung von Gas und Luft in Feuerungen* (Verlag Stahleisen, Düsseldorf, 1937).

For all experiments hydrogen, oxygen, and acetylene were supplied from tanks of compressed gas, while natural gas and air were taken from the lines in the laboratory. No purification of these gases was considered necessary, other than the removal of water vapor from the air by passing it through a calcium chloride trap.

Flowmeters for small rates of gas flow (rates not exceeding 4 to 5 cc per sec.) were calibrated by the method of displacement of water from a graduated vessel. With all flowmeters of larger capacity a wet test meter was employed. Because of the comparatively high solubility of acetylene in water, neither of the foregoing methods of calibration was applicable to this gas. Therefore, a system was devised by which a volume of acetylene could be withdrawn from the tank, measured, and then displaced under constant pressure through the flowmeter by water that was maintained saturated with acetylene gas.

In all calibrations the pressure at the exit of the flowmeter was atmospheric. During the experiments the exit pressure generally rose a few

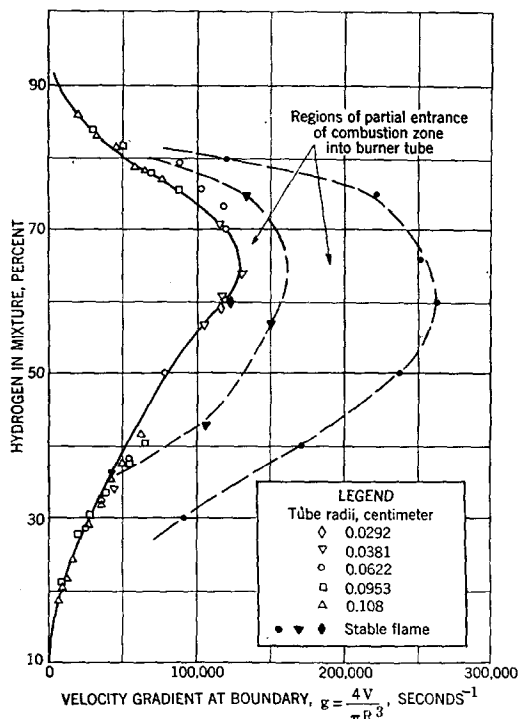


FIG. 8. Critical velocity gradients at boundary of gas stream for flashback of hydrogen-oxygen flames in cylindrical water-cooled tubes of different diameters.

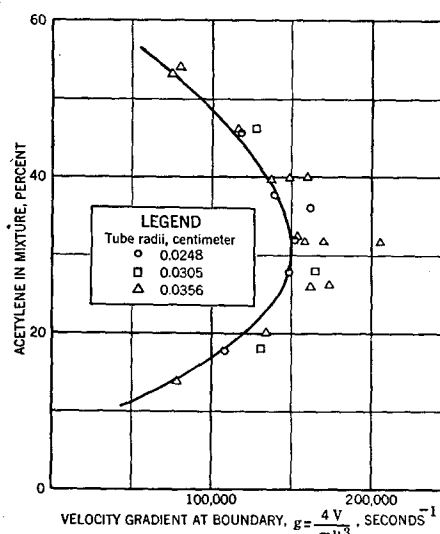


FIG. 9. Critical velocity gradients at boundary of gas stream for flashback of acetylene-oxygen flames in cylindrical water-cooled tubes of different diameters.

mm Hg above atmospheric pressure because of the flow resistance of the mixing chamber and the burner tube, and corrections became necessary to reduce the flowmeter readings to volumes delivered at the burner port. Theoretically, if the flow through the meter follows Poiseuille's law, the volume passing through the capillary per unit time at a given scale reading is independent of pressure; hence, the volume delivered at the port is increased by the factor  $(1 + \Delta P/P_{at})$ , where  $\Delta P$  is the excess of pressure above atmospheric at the flowmeter exit and  $P_{at}$  is the prevailing atmospheric pressure. If the constriction of the flowmeter consists of a plate orifice, the volume passing through the orifice per unit time at a given scale reading is proportional to the inverse of the square root of the pressure at the meter entrance (see, for example, Whitwell<sup>9</sup>) and hence, the volume delivered at the port is increased approximately by the factor  $(1 + \Delta P/P_{at})^{1/2} \approx 1 + \frac{1}{2} \Delta P/P_{at}$ . Tests have shown that, for the square-cut capillaries used in this work, the correction factor could be written as  $1 + \gamma \Delta P/P_{at}$ , where for air, oxygen, and acetylene,  $\gamma = 0.5$ , and for hydrogen,  $\gamma = 0.8$ .

Pyrex-burner tubes were used for the series of experiments with hydrogen-air mixtures. For mixtures of hydrogen and oxygen, tubes of

<sup>9</sup> J. C. Whitwell, Ind. Eng. Chem. **30**, 1157 (1938).



Pyrex and a porcelain thermocouple tube with an inside diameter of 0.0584 cm were used. The burner tubes for acetylene-oxygen flames were made by drilling holes of 0.049 to 0.071 cm diameter in brass rods. To provide for laminar gas flow at the orifice, the length of any burner tube was at least 40 times its inner diameter.

Determinations of limits of inflammability between plane parallel plates for natural gas-air mixtures of 6.0 to 11.5 percent natural gas were made with the use of a rectangular metal burner whose cross section was of 1.6-cm length and of adjustable width. The limiting width for the downward propagation of a given mixture was measured with a micrometer. Inflammability limits were redetermined in a cylindrical tube of known diameter and compared with older data to preclude errors arising from possible changes in natural gas composition.

The pressures developed in the acetylene-oxygen flames were measured by a water barometer, which, at one side, was attached to the burner tube just below the orifice, and open to the atmosphere at the other side. A continuous flow of water through the jacket surrounding the burner tip was required in order to obtain constant values.

### (B) Ranges of Flashback and Flame Tilt

From the values of the flow rates at which instantaneous—or true—flashback of hydrogen-air and hydrogen-oxygen flames occurred, the velocity gradients at the wall may be calculated. Plots of the critical velocity gradient *versus* mixture composition for these two types of flames (solid curves, Figs. 7 and 8) show the behavior expected theoretically, that is, the velocity gradient for flashback of a flame of a given mixture composition is independent of the

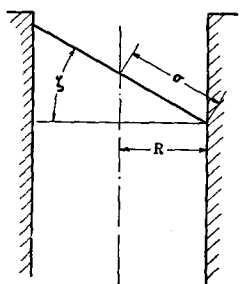


FIG. 10. Idealized combustion zone of tilted flame.

TABLE I. Calculation of  $K$  at the limit of the tilted flame range for various gas mixtures.

$R$ cm	$g$ sec. <sup>-1</sup>	$K \times 10^{-3}$ , sec. <sup>-1</sup>
9 percent natural gas + 91 percent air; $S_u = 38$ cm/sec.		
0.775	652	0.78
0.709	504	0.67
0.649	493	0.68
0.534	494	0.65
0.440	433	0.96
34 percent hydrogen + 66 percent air; $S_u = 230$ cm/sec.		
0.226	18,100	21
0.147	14,600	19
0.108	13,500	22
60 percent hydrogen + 40 percent oxygen; $S_u = 790$ cm/sec.		
0.0622	265,000	300
0.0381	158,000	230
0.0292	122,000	360

tube diameter. However, the foregoing flashback data lose their practical significance because the regions of tilted flame, shown by the areas between the dotted and solid curves of Figs. 7 and 8, become much more extensive than is the case with natural gas-air flames. Actually these regions constitute a continuation of the range of unstable flame, inasmuch as the development of a tilted flame is followed invariably by flashback except for very lean or rich mixtures.

Flashback induced by flame tilt, as distinguished from the instantaneous phenomenon, is rather easily recognized with hydrogen flames. While hydrogen-air flames are not distinctly visible because of their low luminosity, the existence of tilt, though short-lived, can be observed in a shadow picture of the flame; with hydrogen-oxygen flames, the brilliance and pinpoint smallness of the cone often obscures the partial entrance of the flame into the tube, but a time-lag is observed between the formation of a flame and flashback. Rich flames of acetylene-oxygen mixtures may be drawn into the tube at several places around the rim, thus giving rise to a pronged flame which sometimes rotates because the points of entry of the flame shift from time to time. Since, as discussed below, the process of ignition induces flashback in acetylene-oxygen mixtures at flows considerably exceeding the true flashback limit, these mixtures were first ignited at flows far within the stable flame range, and the flow was then reduced until flashback occurred. In this process the flame

became strongly tilted and tended to flash back on slight disturbances; therefore, the flashback limits shown in Fig. 9 probably represent the lowest obtainable limits induced by tilted flames, and the region of true flashback cannot be outlined exactly.

On the whole, the partial entrance of the combustion zone into the burner tube is a more complicated phenomenon in acetylene-oxygen flames than in other flames. The limits of the tilted flame range could not be reproducibly established. They seemed to depend largely on fortuitous changes in the contour of the burner port. The intense heat and the radial gas flow at the flame base (cf. Fig. 5) melted away the original sharp edge of the tube and formed an irregular recess around the port.

Since tilted flames are formed by partial flashback, it appears that, above some limiting value of the gradient  $g$  of gas velocity at the tube wall, tilted flames cannot be formed. However, this limiting value changes with tube diameter, since the phenomenon depends on the deflection of the

flow lines, that is, the pressure that the combustion zone exerts normal to the tube axis. If the combustion zone is assumed to be a plane surface within the burner tube, as shown in Fig. 10, the component of pressure normal to the tube axis may be taken proportional to the sine of the angle  $\zeta$ ; and, at the limit of the tilted flame range, the ratio  $g/\sin \zeta$  may be expected to remain the same for a given mixture composition in tubes of different diameters. From geometrical relations

$$\sin \zeta = \left(1 - \frac{R^2}{\sigma^2}\right)^{\frac{1}{2}} = \left(1 + \frac{R}{\sigma}\right)^{\frac{1}{2}} \cdot \left(1 - \frac{R}{\sigma}\right)^{\frac{1}{2}}, \quad (3)$$

where  $\sigma$  is the major semi-axis of the elliptical combustion zone of area  $\pi\sigma R$ . Since the ratio  $R/\sigma$  is of a magnitude comparable to 1, Eq. (3) becomes approximately

$$\sin \zeta = 1.4 \left(1 - \frac{R}{\sigma}\right)^{\frac{1}{2}}. \quad (4)$$

Equating the gas flow  $V$  with the gas flow through

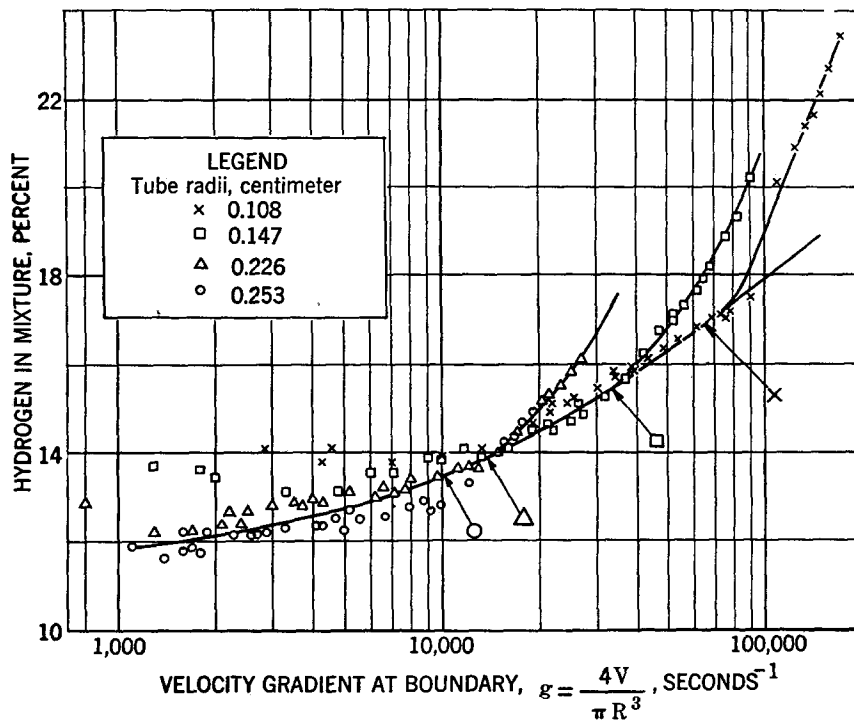


FIG. 11. Critical velocity gradients at boundary of gas stream for blow-off of hydrogen-air flames in cylindrical water-cooled tubes of different diameters. Arrows with symbols mark the beginning of turbulent flow (Reynold's number 2200) in the tubes corresponding to the symbols.

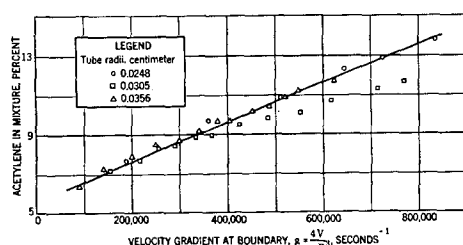


FIG. 12. Critical velocity gradients at boundary of gas stream for blow-off of acetylene-oxygen flames in cylindrical water-cooled tubes of different diameters.

the combustion zone

$$V = \pi \sigma R S_u, \quad (5)$$

where  $S_u$  is taken to be constant over the zone. Substituting Eq. (1) in (5) and transforming

$$R/\sigma = 4S_u/gR, \quad (6)$$

and the condition that, at the limit of the tilted flame range,  $g/\sin \zeta$  remains constant, may be written

$$\frac{g}{(1 - 4S_u/gR)^{1/2}} = K. \quad (7)$$

Table I contains numerical values of  $K$  for the various gas mixtures investigated. The data for natural gas-air mixtures are taken from Lewis and von Elbe.<sup>4,10</sup> The burning velocities for hydrogen mixtures are taken from Jahn.<sup>7</sup> The constancy of the  $K$  values is satisfactory.

### (C) Range of Blow-off

Figures 11 and 12 show the critical velocity gradients for blow-off of hydrogen-air and acetylene-oxygen flames. The hydrogen-oxygen flames have not been investigated because their blow-off curves generally fall outside the laminar flow range. This is also largely true for hydrogen-air flames. Since Eq. (1) for the velocity gradient is valid only for laminar flow, the extension of this equation to the range of turbulent flow yields values of  $g$  of obscure physical significance that form curves branching off the main laminar flow curve. By combining Eq. (1) with the equation

<sup>10</sup> The apparent anomalous extrusion of the  $g_F$  curve for a tube of 1.550-cm diameter (cf. reference 4, Figs. 8a and 11) has been recognized to belong to the tilted-flame range.

for the Reynolds number,

$$2\rho V/\pi\eta R = 2200, \quad (8)$$

the gradient  $g_t$  at the point of transition from laminar to turbulent flow is found to be

$$g_t = 2\eta(2200)/R^2\rho. \quad (9)$$

It is seen that each curve of Fig. 11 undergoes a pronounced change in slope at the value of  $g_t$  (indicated by arrows in the figure), computed for the corresponding tube.

Figure 11 also shows that the critical velocity gradients for blow-off become dependent on the tube diameter when the diameter and the gas flow are very small. Under these conditions the quenching effect of the port rim penetrates into the interior of the stream beyond the linear range of the gas velocity curve; therefore, blow-off is attained with a smaller velocity gradient.

TABLE II. Pressure difference between unburned gas and atmosphere for acetylene-oxygen flames.

Acetylene in mixture percent	Total gas flow cc/sec.	Flame pressure cm H <sub>2</sub> O
Inside diameter of burner tube, 0.049 cm		
18.0	6.0	2.0
28.0	6.0	5.2
46.0	6.0	3.4
Inside diameter of burner tube, 0.061 cm		
14.0	4.0	1.2
	8.0	0.9
	12.0	1.2
		Av. 1.1
18.0	6.0	2.4
	9.0	2.3
	12.0	2.5
		Av. 2.4
23.0	6.0	3.4
	9.0	3.4
	12.0	3.6
		Av. 3.5
28.0	8.0	5.0
	10.0	5.3
	11.0	5.4
	12.0	5.2
	14.0	5.7
		Av. 5.3
36.0	6.0	5.6
	9.0	5.4
	12.0	5.5
		Av. 5.5
46.0	6.0	3.4
	8.0	3.3
	10.0	3.7
		Av. 3.5
52.0	4.0	1.3
	5.0	1.5
	6.0	1.5
	8.0	1.7
		Av. 1.5

TABLE III. Calculated temperatures and density ratios for acetylene-oxygen flames of various mixture compositions. ( $T_u = 291^\circ\text{K}$ ,  $P = 1$  atmos.)

C <sub>2</sub> H <sub>2</sub> in mixture, percent	CO	CO <sub>2</sub>	Mole fraction of reaction products at equilibrium		H <sub>2</sub> O		H <sub>2</sub>	H	$T_b$ ( $^\circ\text{K}$ )	$\rho_u/\rho_b$
			O <sub>2</sub>	O	OH					
14.0	0.084	0.183	0.471	0.075	0.098	0.074	0.005	0.011	2980	10.75
28.6	0.326	0.118	0.099	0.113	0.144	0.078	0.026	0.090	3303	14.61
35.7	0.441	0.076	0.028	0.076	0.118	0.073	0.057	0.127	3366	15.95
45.5	0.556	0.021	—	0.021	0.035	0.035	0.135	0.198	3357	18.13
50.0	0.600	—	—	—	—	—	0.206	0.194	3288	18.83

An equivalent statement is that, for a given velocity gradient, flames of richer mixtures can be blown off in small tubes. This is illustrated by the lower part of Fig. 11, where the critical gradients for blow-off in small tubes lie above those determined in larger tubes.

#### (D) Flame Pressure and Burning Velocity

The pressure difference on both sides of the combustion zone that is caused by the mass acceleration within the zone is given by the equation<sup>5</sup> (cf. Lewis and von Elbe):<sup>11</sup>

$$p_u - p_b = \Delta p = \rho_u S_u^2 (\rho_u / \rho_b - 1). \quad (10)$$

The pressure  $p_u$  represents essentially the pressure throughout the whole stream of unburned gas because the pressure gradient along the burner tube is very small;  $p_b$  is substantially identical with the pressure of the surrounding atmosphere, so that  $\Delta p$  may be taken as the pressure difference between the gas in the burner tube and the outer atmosphere.

For natural gas-air mixtures the flame pressure  $\Delta p$ , calculated from values of  $S_u$  and  $\rho_u/\rho_b$ ,<sup>4</sup> is only 0.01 cm of water for the strongest mixture; on the other hand, for acetylene-oxygen mixtures, pressures up to 5.5 cm of water are observed. This is shown in Table II. The resulting compression of an acetylene-oxygen mixture in the burner and connecting tubes at the instant of ignition slows down the gas stream momentarily to such an extent that flashback occurs over a considerable range of gas flows that would otherwise yield stable flames. In determining the flashback point, it is therefore necessary to ignite the mixture at a much higher flow, and to reduce the flow gradually until flashback occurs.

Since the pressures of acetylene-oxygen flames can be measured conveniently and rather accurately, they may be used to calculate the burning velocities. For this purpose,  $\rho_u/\rho_b$  is calculated from the equation:

$$\rho_u/\rho_b = \frac{\Sigma m_b T_b}{\Sigma m_u T_u}, \quad (11)$$

where  $\Sigma m$  is the total number of moles and  $T$  the absolute temperature. No correction is required for the small pressure difference between burned and unburned gas. Values of  $\Sigma m_b/\Sigma m_u$  and  $T_b$ ,

TABLE IV. Inner cone dimensions and burning velocities calculated from cone areas of acetylene-oxygen flames.

Acetylene in mixture percent	Total gas flow cc/sec.	Cone base, mm	Cone height, mm	Cone area mm <sup>2</sup>	Burning velocity ( $S_u$ ) cc/sec.
Inside diameter of burner tube, 0.049 cm					
18.0	6.0	0.858	1.330	1.89	318
	8.0	0.779	1.759	2.21	363
	10.0	0.771	2.083	2.57	389
28.0	6.0	0.761	1.112	1.41	427
	8.0	0.731	1.374	1.63	490
	10.0	0.717	1.697	1.96	515
36.0	6.0	0.782	1.149	1.49	402
	8.0	0.873	1.461	2.09	383
	10.0	0.784	1.737	2.19	456
Inside diameter of burner tube, 0.071 cm					
14.0	12.0	0.959	1.954	3.03	396
	16.0	0.985	2.550	4.02	398
18.0	9.0	0.859	1.288	1.83	491
	12.0	0.945	1.588	2.46	488
	15.0	0.905	2.006	2.92	514
23.0	12.0	1.015	1.362	2.32	518
	15.0	1.022	1.771	2.96	507
	18.0	1.078	2.090	3.70	493
36.0	15.0	1.041	1.650	2.83	530
	20.0	1.028	2.112	3.51	570
46.0	12.0	1.192	1.650	3.29	365
	15.0	1.116	1.999	3.64	384
52.0	10.0	1.080	1.815	3.21	312
	13.0	1.131	2.210	4.05	321

<sup>11</sup> B. Lewis and G. von Elbe, *Combustion, Flames, and Explosions of Gases* (Cambridge University Press, 1938), pp. 202-3.

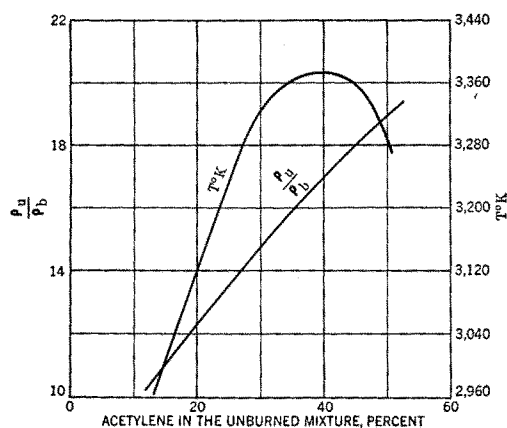


FIG. 13. Ratio of densities,  $\rho_u$  and  $\rho_b$ , of unburned and burned gas and absolute temperature of acetylene-oxygen flames. Initial temperature 291°K, pressure = 1 atmos.

for  $T_u = 291^\circ\text{K}$  and atmospheric pressure, are calculated thermodynamically, as described elsewhere,<sup>12</sup> with all possible dissociation equilibria considered. The results are summarized in Table III and Fig. 13. For mixtures of 50 percent to 28.6 percent acetylene, the calculations are given by Montagne.<sup>13</sup> Since these calculations do not extend to leaner mixtures, the calculation for the 14 percent mixture is added.

The usual method of determining burning velocities, as originally proposed by Gouy, consists in measuring the area  $F$  of the inner cone and the gas flow  $V$ ; taking the gas flow normal to the combustion zone as  $S_u \times F$ , one obtains

$$S_u = V/F, \quad (12)$$

where  $S_u$  represents an average value from tip

<sup>12</sup> Reference 11, pp. 285-93.

<sup>13</sup> M. P. Montagne, *Chaleur et Industrie* 19, 54 (1938).

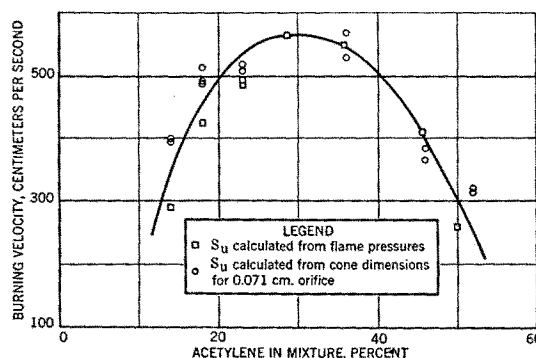


FIG. 14. Burning velocity curve for acetylene-oxygen mixtures.

to base. It is hardly worth while to determine the cone area precisely; instead,  $F$  may be calculated from the cone height  $h$  and the radius  $R'$  of the base by the equation for the right circular cone

$$F = \pi R' (R'^2 + h^2)^{1/2}. \quad (13)$$

Table IV contains values of  $2R'$  and  $h$ , measured by means of a cathetometer, for various acetylene-oxygen flames. It may be noted that in flames of this type the diameter of the cone base considerably exceeds the tube diameter. Constant values are obtained with a burner tube of 0.071-cm diameter, while in the smaller tube of 0.049-cm diameter, the gas flow appreciably affects the results, indicating a considerable influence of the port rim. Figure 14 shows the values of  $S_u$  obtained from flame pressures and cone dimensions, respectively; although the two methods are profoundly different, the results agree very well with each other.